

SUPPORTING INFORMATION

Early Pleistocene vegetation change in upland south-eastern Australia

J.M.K. Sniderman

Journal of Biogeography

Appendix S1 Additional site details and analyses (Figs S1–S5 and Table S1).

Figure S1: Stony Creek Basin locality diagram.

Figure S2: Stratigraphy and lithology of the Stony Creek Basin core.

Figure S3a-f: Detailed Stony Creek Basin pollen diagram.

Figure S4: Stratigraphic distribution of pollen types observed in clumps of ≥ 2 grains.

Figure S5: Group-average cluster analysis dendrogram of Stony Creek Basin pollen spectra, terminals labelled by sample depth.

Figure S6: Group-average cluster analysis dendrogram of mean palynological composition of Stony Creek Basin zones, terminals labelled by zone.

Table S1: Pearson's correlation coefficients between charcoal and major pollen types and rate of change.

Figure S1: Stony Creek Basin locality diagram.

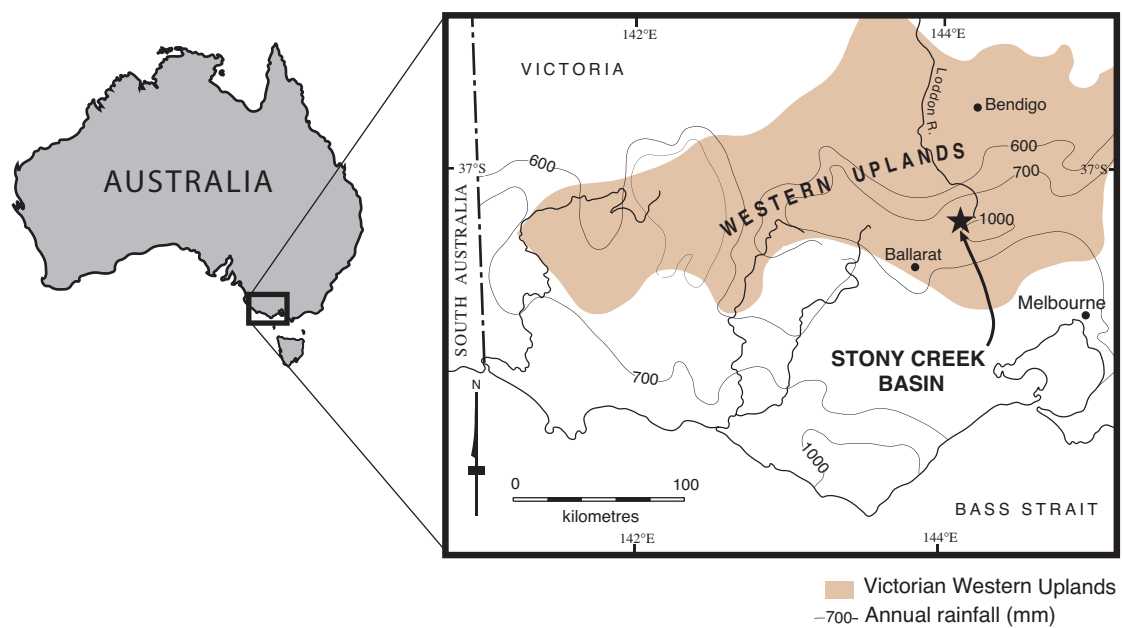


Figure S2: Stratigraphy and lithology of the Stony Creek Basin core recovered in 2000. Left column, core recovery (black, recovered core; white, core gaps); right column, sediment lithology. Sediments are predominantly black silty clays. Sediments from 0-3880 cm below the surface were predominantly black to very dark grey silty clays, massive or finely laminated, with slightly paler colours where laminated. One major exception to the monotonous silty clay lithology was an eight cm thick horizon at 2889-2897 cm, of poorly sorted gravelly sandy silt, incorporating clasts 1-2 mm and up to 6 mm. Lithics within this horizon included siltstone and sandstone, and milky and clear quartz, the latter both rounded and conchoidally fractured. Following sieving and weight separation of samples of this horizon, dissecting microscope petrology revealed a heavy mineral fraction of sharp-fractured chrome spinel, ilmenite, and zircons (J. Hollis, Australian Museum, unpublished data). Because of its poor sorting, sharply fractured minerals and lithics, and distinctive mineral composition, this horizon was interpreted as a pyroclastic deposit. Below 3880 cm, the black silty clays graded downward into bedded and strongly laminated grey sandy silts. Sniderman *et al.* (2007) presented fission track analyses of zircons recovered from near the base of this horizon, and from the pyroclastic deposit at 2889-2897 cm.

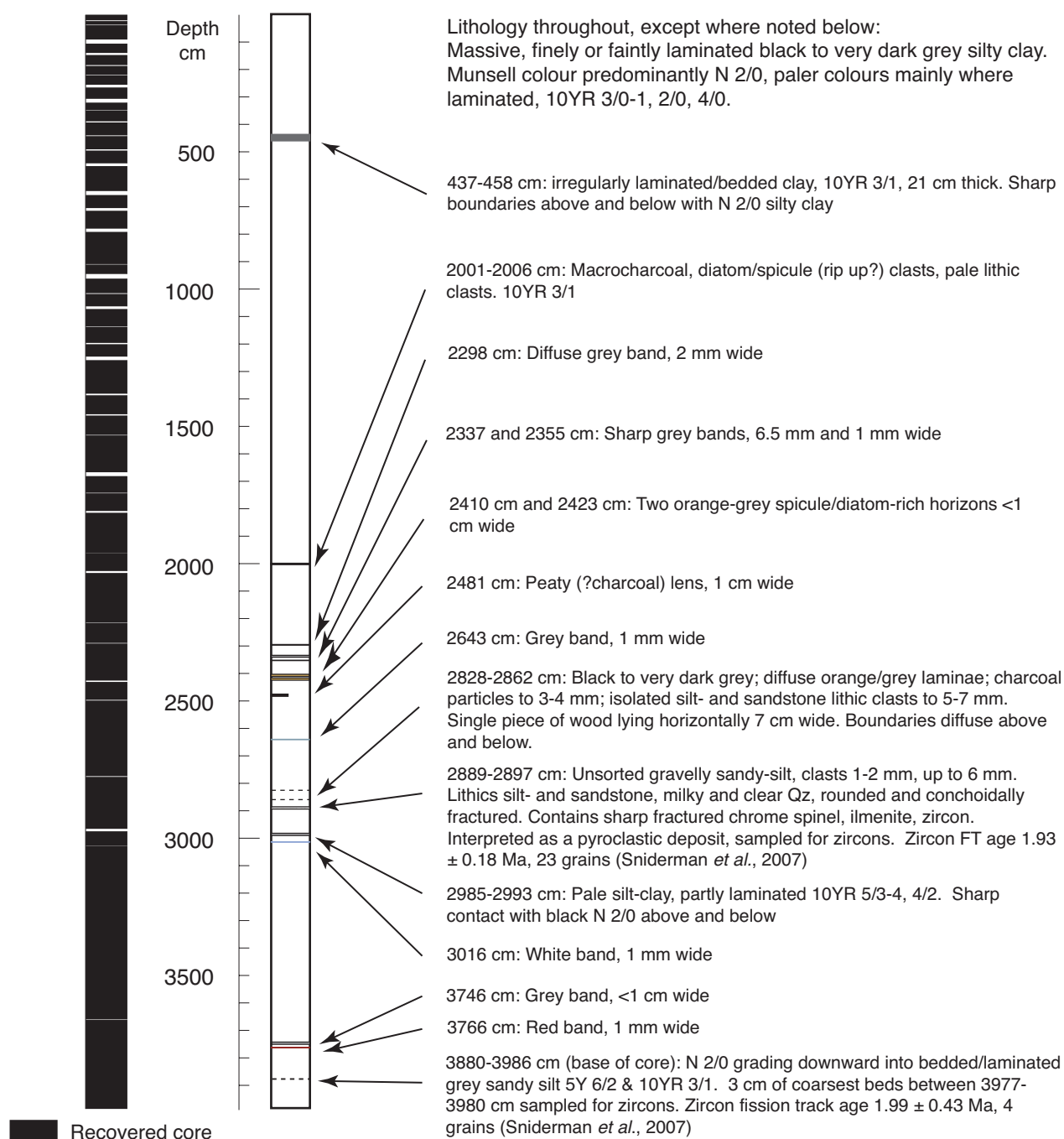


Figure S3a-f Detailed Stony Creek Basin pollen diagram, plotted by depth. (a) rain forest gymnosperms and rain forest angiosperms.

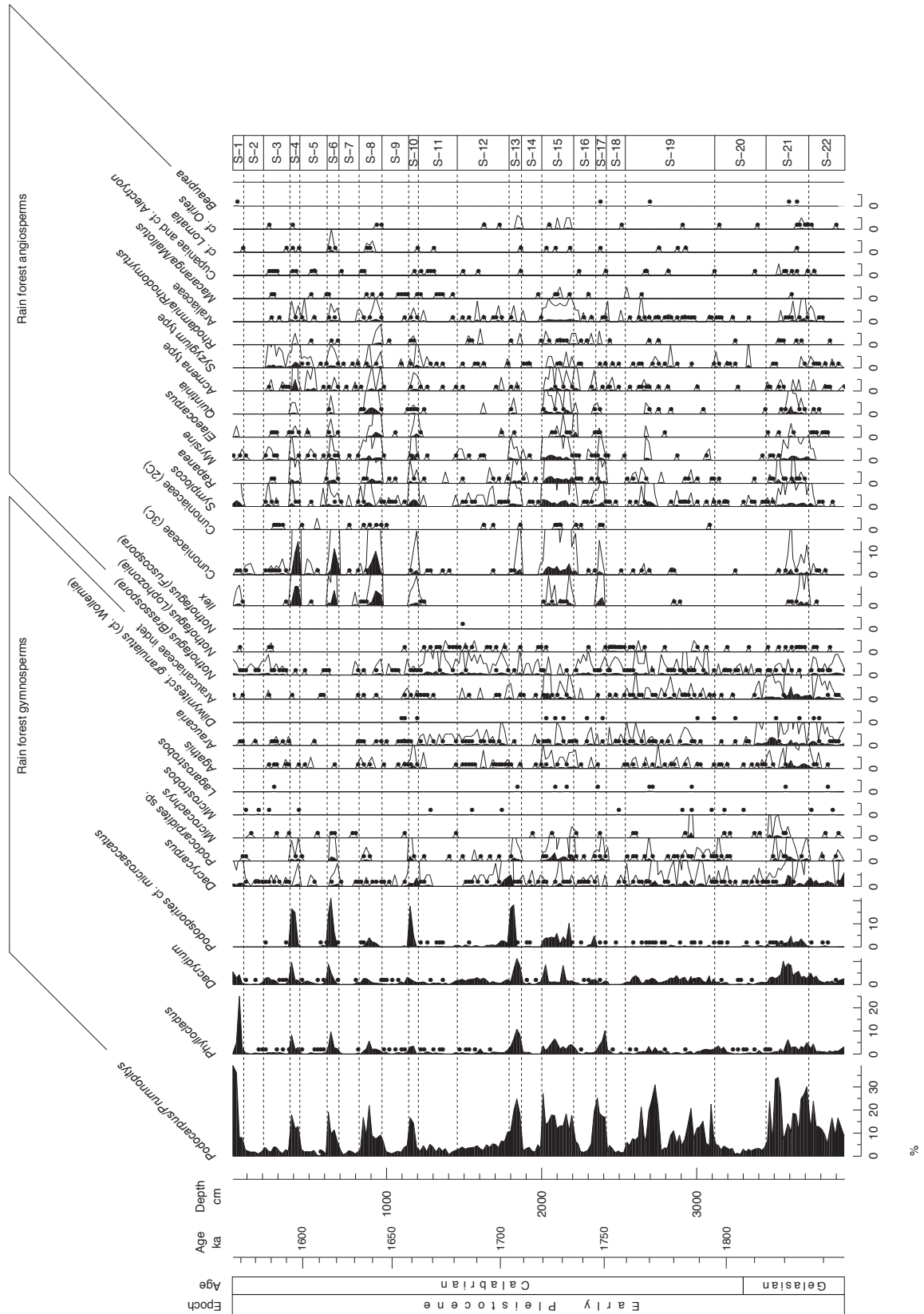


Figure S3a-f Detailed Stony Creek Basin pollen diagram, plotted by depth. (c) open forest taxa.

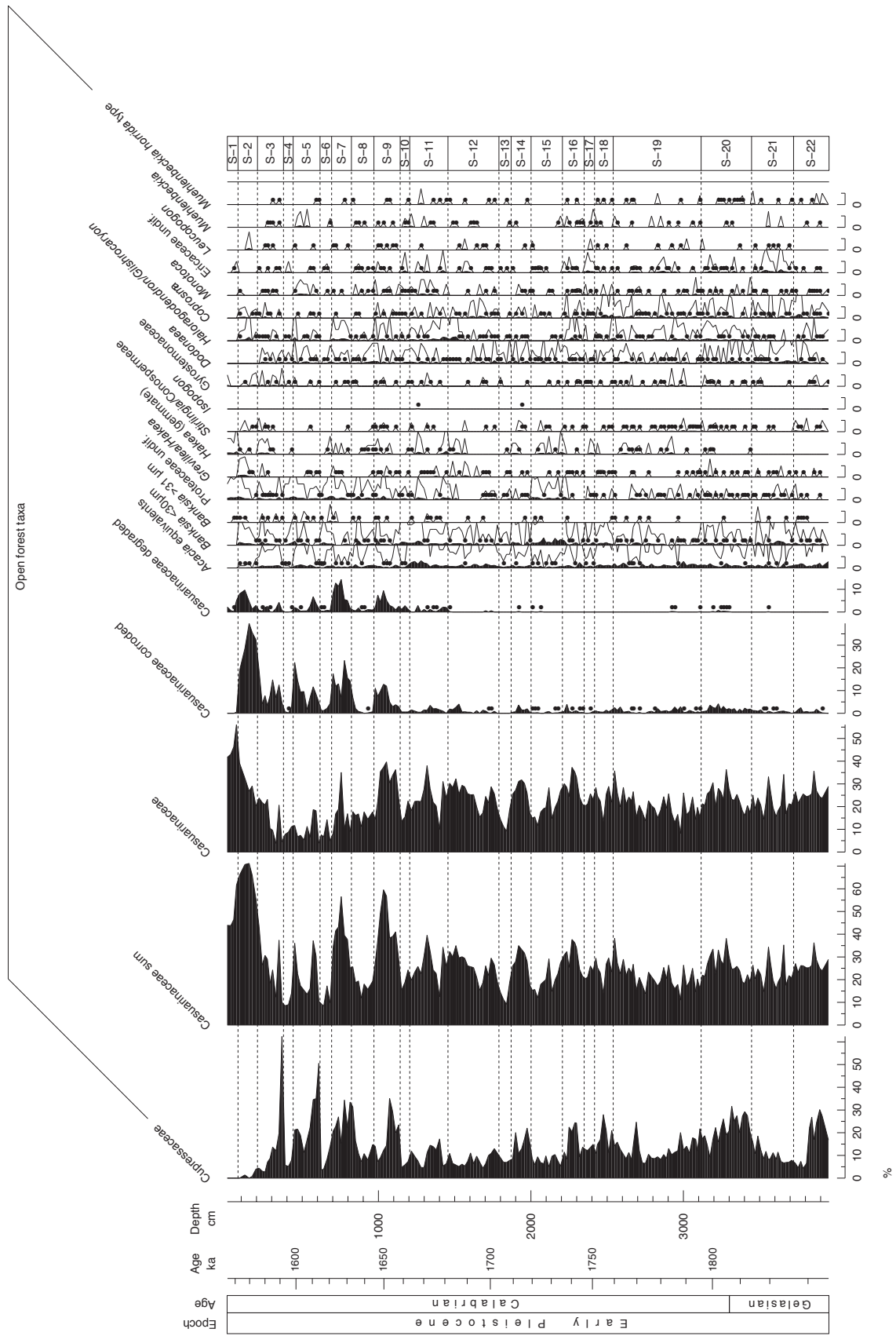


Figure S3a-f Detailed Stony Creek Basin pollen diagram, plotted by depth. (e) pteridophytes, other spores, and aquatic taxa.

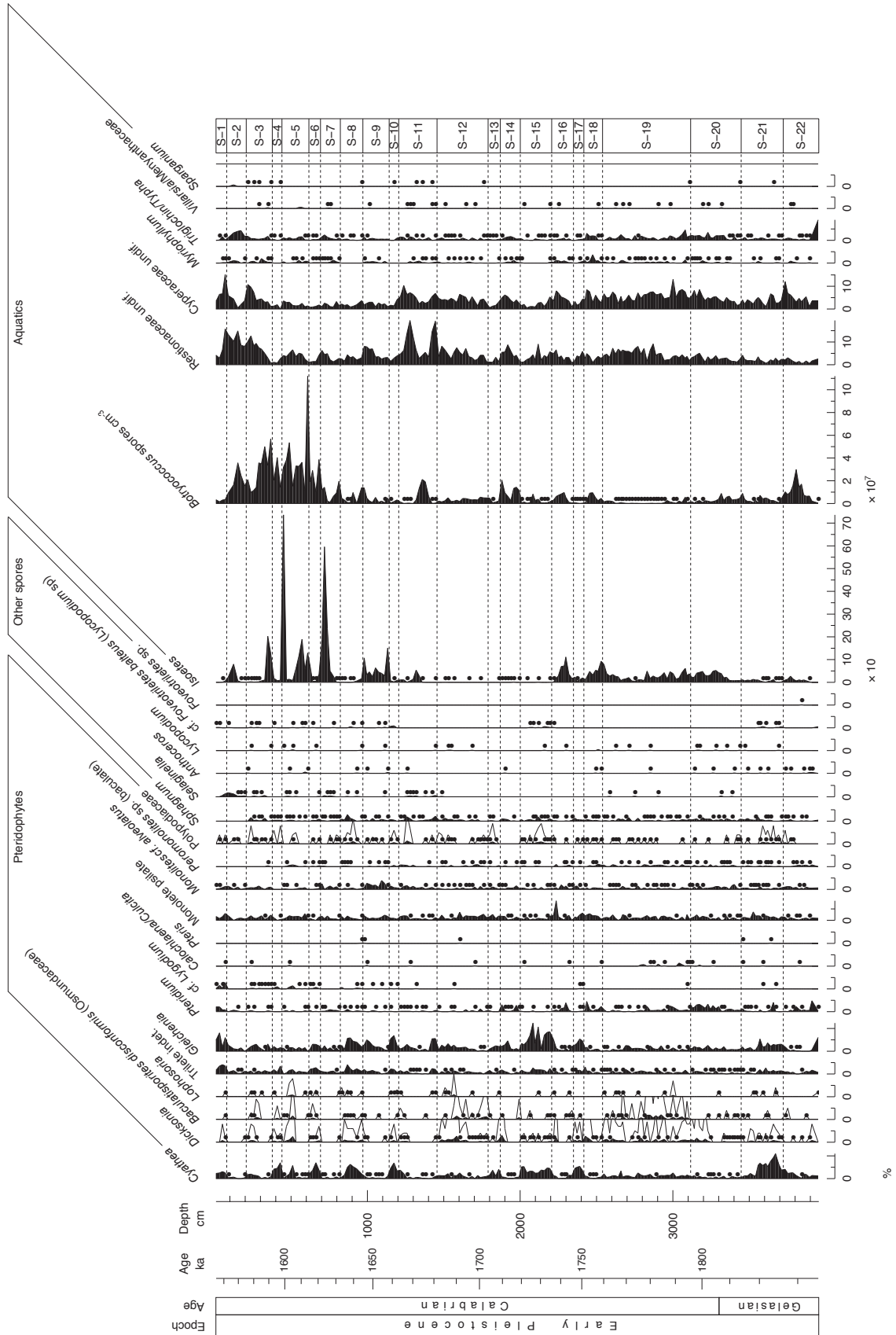


Figure S3a-f Detailed Stony Creek Basin pollen diagram, plotted by depth. (f) deteriorated and unknown pollen, charcoal and pollen concentrations, a charcoal:pollen ratio, and sediment organic matter content (loss on ignition).

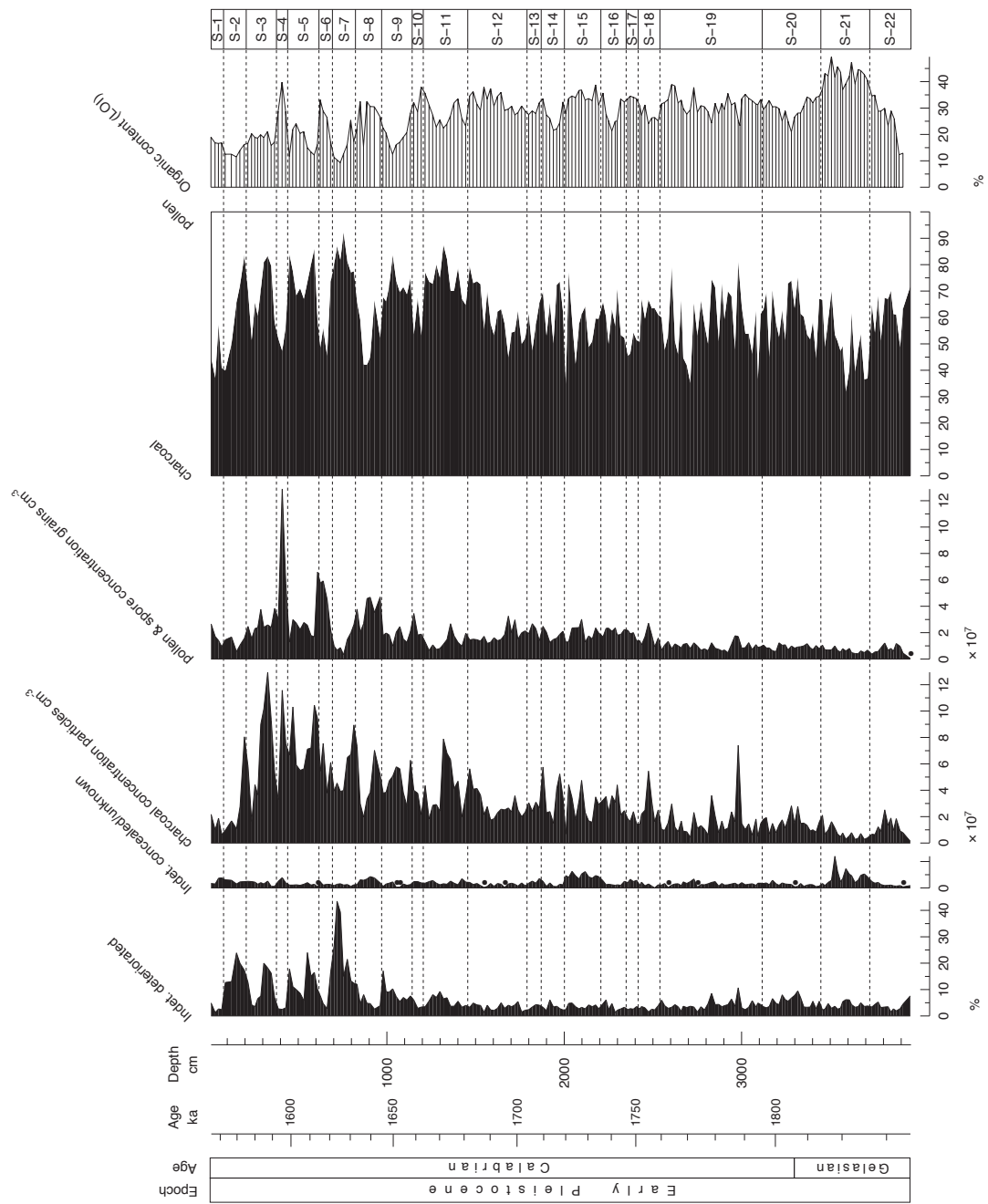


Figure S5: Group-average cluster analysis dendrogram of Stony Creek Basin pollen spectra, terminals labelled by sample depth.

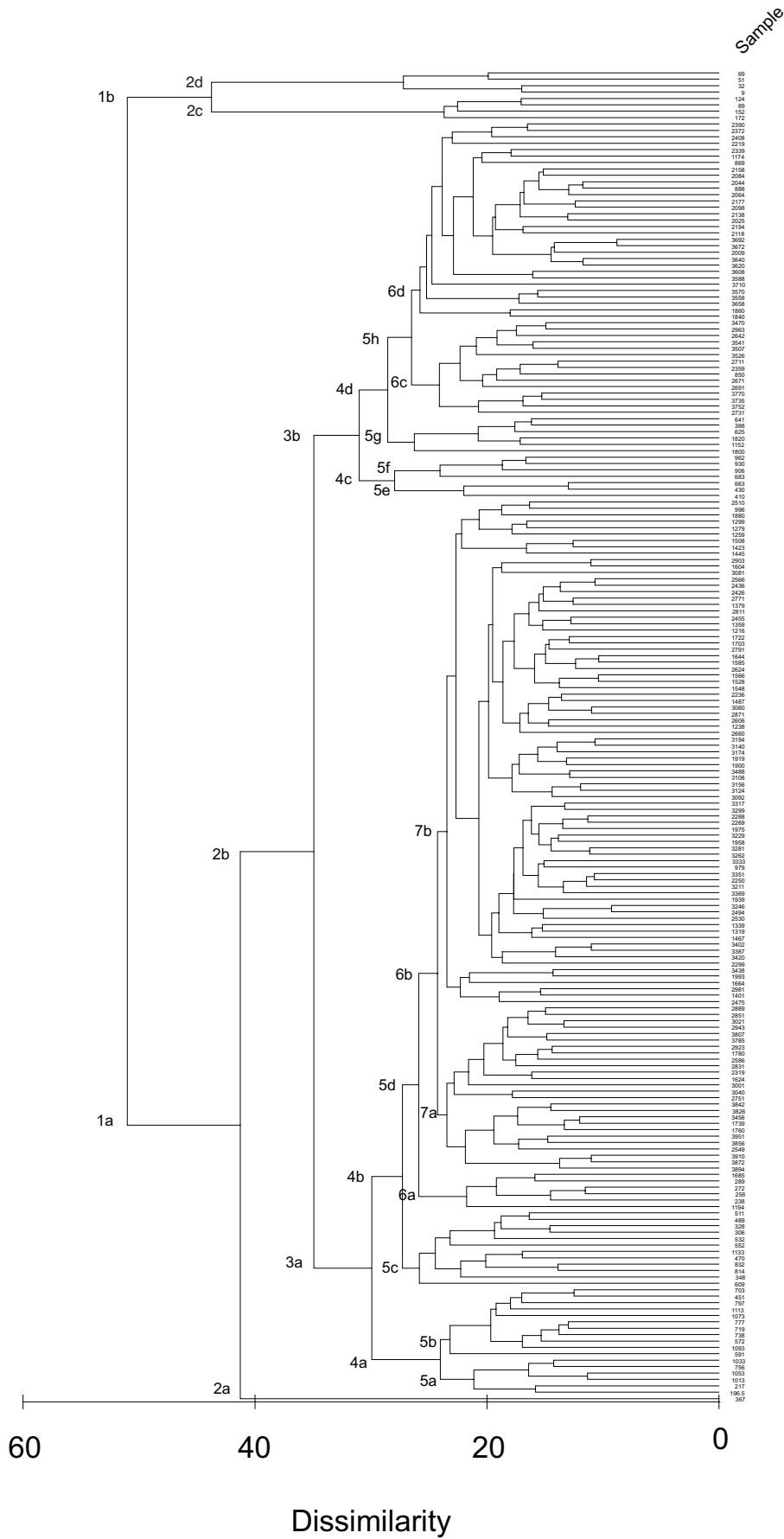


Figure S6: Group-average cluster analysis dendrogram of mean palynological composition of Stony Creek Basin zones, terminals labelled by zone.

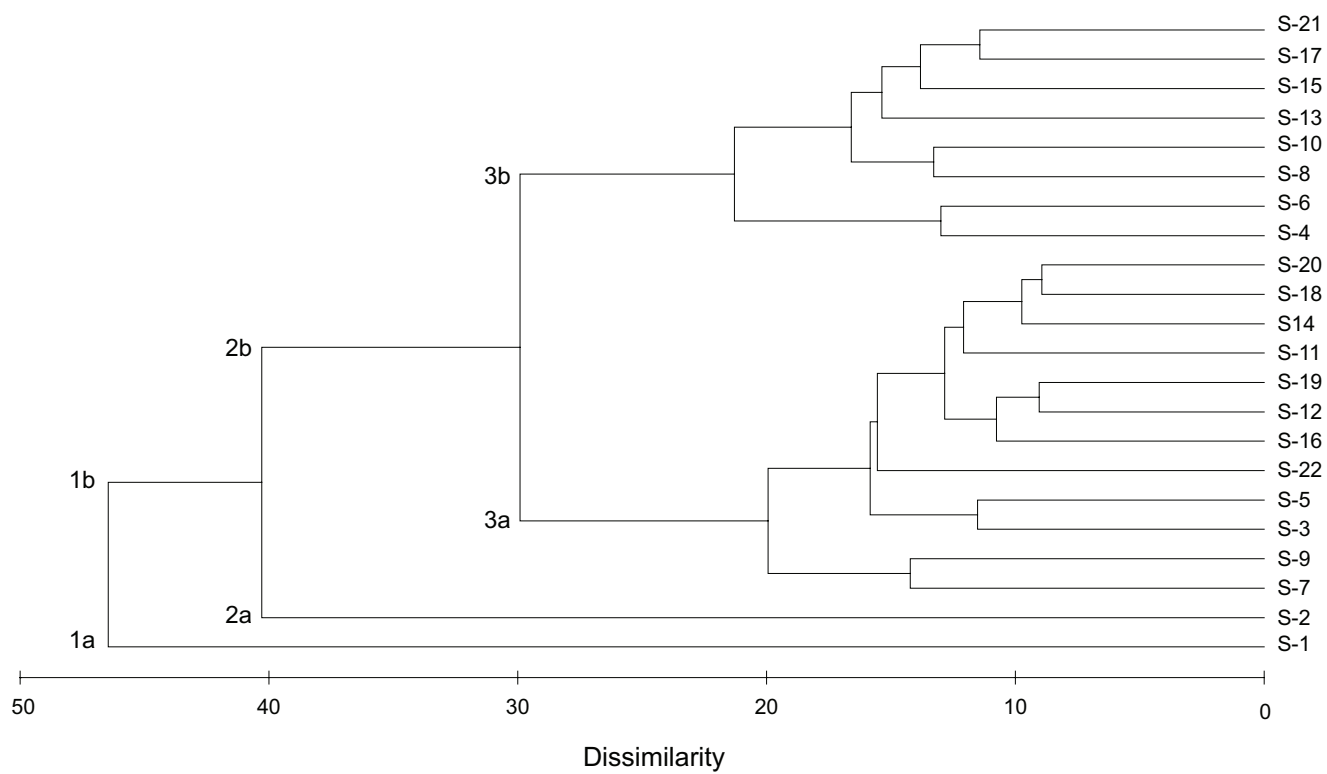


Table S1: Pearson's correlation coefficients between charcoal and major pollen types and rate of change. Correlations significant at the 0.05 level are highlighted in bold. Before correlations, all time series were smoothed (3 point arithmetic smooth, with weights 1:2:1), the uppermost eight samples were omitted because of strong taphonomic biases, then detrended.

	charcoal
<i>Eucalyptus</i>	-0.2126 <i>P</i> = 0.0026
<i>Callitris</i>	0.4464 <i>P</i> < 0.001
Casuarinaceae	-0.2460 <i>P</i> = 0.005
Rainforest angiosperms	-0.0444 <i>P</i> = 0.5335
Podocarpaceae	-0.1194 <i>P</i> = 0.0929
Rate of change	0.2976 <i>P</i> < 0.001